Journal of Radioanalytical and Nuclear Chemistry (2020) 326:393–405
https://doi.org/10.1007/s10967-020-07279-2

Uranium speciation and distribution in *Shewanella putrefaciens* and anaerobic granular sludge in the uranium immobilization process

Feng-Yu Huang[1] · Hai-Ling Zhang[2] · Yong-Peng Wang[2] · Fa-Cheng Yi[1] · Su Feng[3] · He-Xiang Huang[2] · Meng-Xi Cheng[2] · Juan Cheng[3] · Wen-Juan Yuan[3] · Jie Zhang[3]

Received: 20 April 2020 / Published online: 6 July 2020

Abstract

The uranium (U) in *Shewanella putrefaciens* (*S. putrefaciens*) and anaerobic granular sludge (AnGS) were fractionated, and the contents and forms of U in each fraction were investigated. The functional groups of microorganisms for U binding and the deposition of U in microbial aggregates were also analyzed. Four main approaches were found involved in U immobilization, including biosorption/complexation by microbial cells and their extracellular polymeric substances (EPS), non-reductive biomineralization, bioreduction and intracellular accumulation. Results show that non-reductive biomineralization was found to be dominated in the U(VI) immobilization process. Besides, the contribution of EPS to U removal could not be ignored.

Keywords Uranium · Speciation · Distribution · Extracellular polymeric substances (EPS) · *Shewanella putrefaciens* · Anaerobic granular sludge (AnGS)

Introduction

Uranium (U) contamination in groundwater has been a significant global environmental problem and multidisciplinary studies have been undertaken to solve the problem [1].The traditional methods, like physical or chemical methods [2, 3] might work in removing U in contaminated groundwater, which usually also brought drawbacks, such as difficulties in regenerating media or bringing new chemical pollution [4, 5]. Comparing with these methods, utilizing microorganisms has drawn more and more attention due to its advantages of sufficient raw materials, low cost, high treatment efficiency and environmentally friendly feature [6–8].

Since the first discovery of anaerobic microorganisms capable of reducing U(VI) in the presence of an electron donor [9], there have been extensive studies on the U removal by microorganisms, including pure cultures (such as *mould*, *Sulfate-reducing bacteria*, *Shewanella*) [4, 10–12] and mixed cultures (such as sediment microcosm, anaerobic granular sludge (AnGS)) [13, 14]. Bacteria could potentially affect U migration by various processes. Four basic mechanisms have been reported involved in bacterial immobilization of U, including biosorption, bioaccumulation, biomineralization and bioreduction [4, 15–17]. These mechanisms in the immobilization process is dominated by microbial species, U forms and external environments. Biosorption, biomineralization and intracellular accumulation might be the main mechanisms for U removal when microorganisms were under aerobic conditions, while bioreduction should not be ignored for some microorganisms when they were in anaerobic circumstances [4, 11, 14].The solubility and mobility of U in groundwater would be greatly decreased when soluble U(VI) were reduced to insoluble U(IV).

The formation of needle shaped U precipitates accumulated in the cytoplasm have been mentioned before by several

Feng-Yu Huang and Hai-Ling Zhang have contributed equally to this work.

✉ Fa-Cheng Yi
yfc66@163.com

✉ Su Feng
fengsu_fs@scu.edu.cn

✉ He-Xiang Huang
weiwei@caep.cn

[1] College of Environment and Resources, Southwest University of Science and Technology, Mianyang 621010, Sichuan, China

[2] Institute of Materials, China Academy of Engineering Physics, Jiangyou 621907, Sichuan, China

[3] Key Laboratory of Bio-Resources and Eco-Environment of the Ministry of Education, College of Life Sciences, Sichuan University, Chengdu 610065, Sichuan, China

authors [18, 19], verifying U could be immobilized by cellular uptake. Microorganisms like *Serratia* and *Citrobacter* immobilized U by precipitation with phosphate, which was released when they consumed phosphorous substrates using their phosphatase activity [12, 20]. Recent study also found that U(VI)-phosphate precipitate could be converted into U(IV)-phosphate precipitate when U reducing bacteria coexisted [21].The solubility of U(IV)-phosphate precipitate in water was much smaller, hence, more stable immobilization form of U was created under such two coupled mechanisms. Moreover, microorganisms could produce macromolecules outside their cell walls, termed as extracellular polymeric substances (EPS). As the medium between cells and substances around them, EPS would influence the behavior of surrounding substances, especially poisonous substances like U [22]. A large amount of U was accumulated in the EPS of AnGS in our previous study and the roles of EPS were multiple [23]. As described above, the mechanisms of U immobilization using microorganisms should be various and complicated. Non-redox processes (biosorption, biomineralization and bioaccumulation) and redox processes might be both involved, microbial cells and their EPS might contribute differently to each process. Hence, so far the microbial mechanisms of U immobilization have not been clearly understood yet.

In order to understand the interactions between microorganisms and U in groundwater system and finally enhance the effectiveness of U bioremediation strategies, it is crucial to determine the speciation and distribution of U in microbial aggregates. As known, U could be present in the form of soluble U(VI) ions, U(VI) particles or U(IV) particles in systems like groundwater, while its forms and relevant quantities would vary with environmental conditions including microbial species or even different parts of microbial aggregates. Therefore, effective fractionation and accurate determination of U in microbial aggregates is necessary. *Shewanella putrefaciens* (*S. putrefaciens*), a model dissimilatory metal-reducing bacterium, which has been known for its diversity of metabolic system. A number of studies have been conducted about the interactions with U and its impact on U mobility [24, 25]. AnGS is a microbial consortium habitat that has high anaerobic activity and good biodiversity, and its enriched U(VI)-reducing microorganisms could effectively and stably reduce U(VI) [14, 26]. In this study, *S. putrefaciens* (representing the pure culture) and AnGS (representing the mixed culture) were selected as two typical microorganisms, and the contents and forms of U in these two microbial aggregates were studied, to further explore the microbial mechanisms involved in U immobilization and the contribution of each mechanism to total U removal. This study has important reference value for further understanding the mechanism of U removal in microbial remediation systems.

Experimental

Cultures of *S. putrefaciens* and AnGS

All chemicals used in this study were analytical grade, and all solutions were prepared using Milli-Q water. The *S. putrefaciens* (CICC 22,940) used in this study was purchased from China Center of Industrial Culture Collection. *S. putrefaciens* was cultured in sterilized medium (tryptone, 10 g; yeast extract, 5 g; sodium chloride, 10 g; H_2O, 1 L) at 30 °C. Then, the cells were harvested by centrifugation (6000 rpm, 10 min) after 18 h and washed two times using bicarbonate buffer (15 mM, pH 7; adding 1.3 mM NaCl). The AnGS was obtained from a full-scale upflow anaerobic sludge blanket reactor (Hefei, Anhui, China) treating starch wastewater, then stored anaerobically at 4 °C. The volatile suspended solids (VSS) content of sludge was 65% and the specific acetoclastic methanogenic activity was 350 mg COD/g VSS/day (COD: chemical oxygen demand).

Batch experiments of U immobilization by *S. putrefaciens* and AnGS

All experiments were carried out under nitrogen atmosphere. U(VI) immobilization tests were carried out in 50-mL serum bottles, containing 20 mL synthetic groundwater and leaving 30 mL headspace. The synthetic groundwater was prepared following similar procedures described previously [23]. The synthetic groundwater was boiled for 10 min, and sparged with N_2 to remove dissolved oxygen. After cooling down to room temperature, 1 g L^{-1} $NaHCO_3$ was dosed to adjust the pH to 7.0. Sodium bicarbonate was used as buffer solution, as well as a complexing ligand for U(VI), representing the natural water research complexed state of U in the groundwater [11, 14]. U added in synthetic groundwater was uranyl sulfate ($UO_2SO_4{\cdot}3H_2O$, 99.99%, Hubei Chushengwei Chemical Co., Ltd, China). 0.27-mL aliquots from a 2200 mg L^{-1} stock solution were added for a final concentration of 30 mg L^{-1} U(VI) in each bottle. The electron donors and microorganisms were successively added into the medium to their respective pre-set concentrations. The final concentrations of *S. putrefaciens* and AnGS were respectively 6×10^8 cells mL^{-1} and 1.3 g L^{-1} (VSS). The electron donors for *S. putrefaciens* and AnGS were respectively 10 mM lactate and 10 mM acetate. Before being sealed with butyl rubber stoppers and aluminum tearoff seals, these bottled bioreactors were sparged with nitrogen again to further remove the residual oxygen.

S. putrefaciens tests continuously ran 2 days, while AnGS tests ran 8 days. In previous studies, 2 days and

8 days were proved to have better removal effect on U for *S. putrefaciens* and AnGS, respectively [23, 27]. During the running time, the temperature was controlled at 30 ± 1 °C and 0.5-mL mixed solution was taken at certain intervals. Each experiment was carried out in triplicate.

Fractionation of U in microbial aggregates

Sequential EDTA, $NaHCO_3$ and HNO_3 extraction approach was applied to fractionate the U in the microbial aggregates in our test due to its effectiveness, whose schematic diagram is shown in Fig. 1. Firstly, 0.5-mL sample was periodically extracted from each test solution and centrifuged at 8000 rpm for 5 min, the centrifugation supernatant was filtered through a 0.45 μm filter pinhole. Then, the pellets were washed twice with the 100 mM anaerobic NaCl solution to remove any loosely banded U(VI) on cell surfaces. Secondly, the pellets were resuspended with 0.5 mL anaerobic EDTA solution (1 mM) and sonication extraction was performed for 10 min to extract the U in EPS. The extraction of EPS was usually carried out in 54 mM (2%) EDTA solution, but high concentration of EDTA solution may also complex U(VI) in extracellular cluster aggregates. Therefore, 1 mM EDTA solution was chosen in our experiment, mainly considering that it did not affect subsequent analysis. Thirdly, after being centrifuged at 8000 rpm for 5 min, the residue was resuspended with 0.5 mL anaerobic $NaHCO_3$ solution (100 mM) and left overnight to extract U(VI) in extracellular cluster aggregates. As reported, 1 M $NaHCO_3$was generally used for extraction of U(VI) [28]. However, cell lysis might be caused by 1 M $NaHCO_3$, hence100 mM $NaHCO_3$ was applied in this test based on consideration on extraction efficiency and cell lysis extent. Fourthly, after being centrifuged at 8000 rpm for 5 min, the residue was resuspended with 0.5 mL anaerobic EDTA solution (100 mM) for 4 h to extract U(IV) in extracellular cluster aggregates. As a strong complexation agent, EDTA can dissolve the U(IV) minerals by forming U(IV)-EDTA complexes [29]. Finally, the residue was treated with 0.5 mL HNO_3 (10%) for 4 h to quantify any remaining U that was attributed to intracellular accumulation. The concentrations of U in supernatant ($U_{Supernatant}$), EPS (U_{EPS}), $NaHCO_3$ extracts (extracellular U(VI), $U_{VI\text{-}EX}$),EDTA extracts (extracellular U(IV), $U_{IV\text{-}EX}$) and HNO_3 extracts (intracellular U(IV), U_{IN}) were analyzed by inductively coupled plasma mass spectrometry (ICP-MS) (NEXION 350, Perkin Elmer), and all samples were acidified in 5% HNO_3 previously.

Analysis of U contained particles in EPS extracts by single particle ICP-MS

The soluble and particulate U fractions in the EPS extracts were quantified by single particle ICP-MS, and so did the size distribution of particulate U. In the single particle mode, the signal of the soluble uranyl ions was obviously different from the signal of the U-containing particles. For relatively large EPS-associated U particles (micron-size), microporous membrane with pore size of 0.22 μm was used

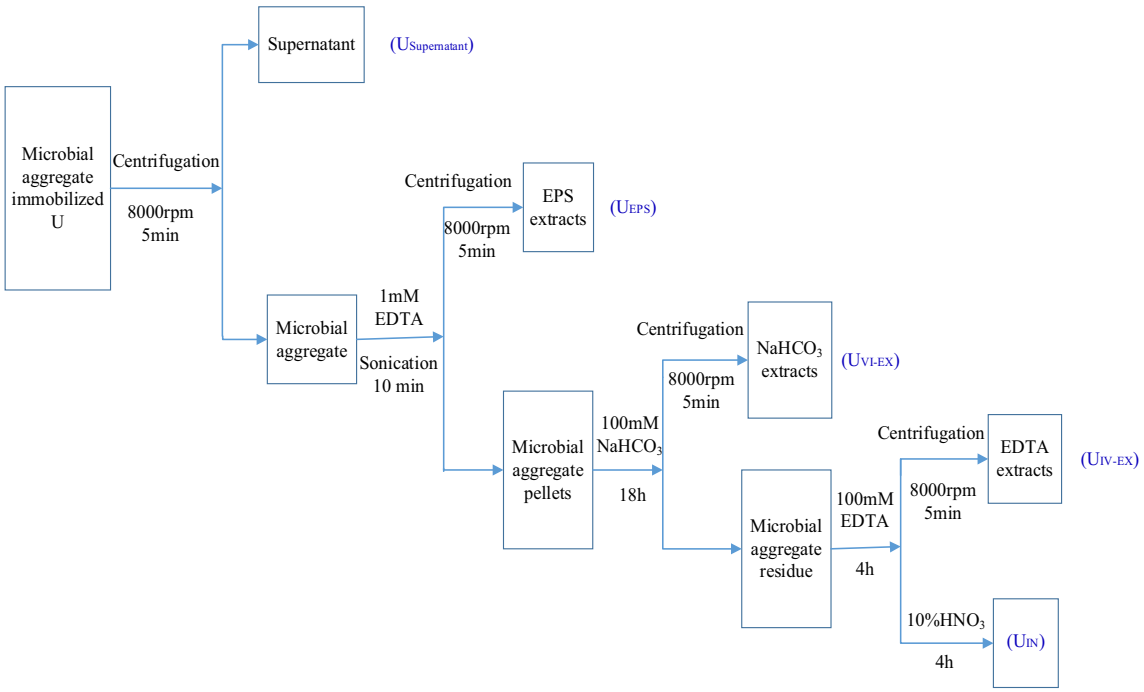

Fig. 1 Schematic diagram for analyses of U in fractionation of microbial aggregates

to differentiate the soluble and particulate U in EPS extracts, as this pore size was proved to be efficient to intercept minerals of size from several microns to tens of microns. After extraction, the EPS samples were filtered through 0.22 µm cellulose nitrate membranes and the initial filtrate was discarded. The difference between the U content in the EPS solution before and after filtration was evaluated to be the mineral fraction of U in EPS (> 0.22 µm).

While for the characterization of size distribution of nanosize U particles, a series of known diameter and particle concentration of silver nanoparticles (Citrate NanoXact™ Silver, nanoComposix Inc.) were used as the standard particle. One colloidal particle could be ionized in the plasma torch to be a flash of ions and displayed as the transient signal to be detected by MS. The signal intensity presents the particle size and the flash frequency accounts the particle concentration.

Analytical methods

Scanning electron microscopy with energy dispersive X-ray (SEM–EDX) and Fourier transform infrared spectroscopy (FTIR) techniques were performed on the microbial aggregates before and after reaction with U. Samples for SEM analysis were briefly fixed in 2.5% glutaraldehyde solution for 4 h, and washed in a phosphate buffer saline followed by a gradual ethanol dehydration series (30%, 50%, 70%, 95% and 100%) for 15 min in turn. Then, the samples were air-dried and pasted on the metal stage with double-sided conductive adhesive, coated with gold before analysis. Finally, the gold-coated samples were examined on Ultra 55 SEM coupled with Oxford IE450X-Max80 EDX. Samples for FTIR spectra were added into KBr powder at a mass ratio of 1:100 and grinded. After dried, a pressed pellet was made by tablet machine. The FTIR spectra were acquired using a Perkin-Elmer Nicolet-5700 spectrophotometer at 4.0 cm^{-1} resolution in the range of 4000–400 cm^{-1}.

Results and discussion

U immobilization using *S. putrefaciens* and AnGS

The time courses of U(VI) immobilization by *S. putrefaciens* and AnGS are shown in Fig. 2. As shown, the content of U in supernatant ($U_{Supernatant}$), the content of U in the microbial aggregates ($U_{total} = U_{EPS} + U_{VI\text{-}EX} + U_{IV\text{-}EX} + U_{IN}$) and the material balance of the system ($U_{system} = U_{total} + U_{Supernatant}$) at each stage of the experiment were analyzed. As time went on, the concentrations of $U_{Supernatant}$ decreased constantly, and the removal efficiency of 92.3% and 96.1% were achieved by *S. putrefaciens* and AnGS, respectively. *S. putrefaciens* cells were cultured to be at the exponential phase with high activity, so the trend of U removal was almost linear during the two-day time course. While for the AnGS, a kind of mixed culture, and taken out from the storage condition of 4 °C for tests, its U reducing activity needed to be recovered and stimulated for a period. Therefore, in the 8-day time course, the U removal by AnGS was small in the first day, then increased almost linearly to Day 3, and finally tended to be stable after three days. In addition, pH in reaction process was measured and found that pH decreased due to the substrate consumption by microorganism. The pH value fallen from 7.0 to 6.2 and 7.0 to 5.7 in *S. putrefaciens* and AnGS test, respectively. After calculating the distribution of U(VI) species at experimental pH range by Visual MINTEQ3.0, U(VI) precipitation could not happen abiotically during the experiment.

The material balance of the two systems during the experiment (U system) is also shown in Fig. 2. Results showed that both two systems could be mass balanced. It is known that biological system is quite complex and the material balance usually could be difficult to be very good. Since S. *putrefaciens* was present as flocs, the material balance was better. While AnGS was granules with particle size from 1 mm to 2 mm, the difficulty in homogeneity sampling of AnGS lead to poorer balance. Whatever, the material balance is within the acceptable level in microbial system.

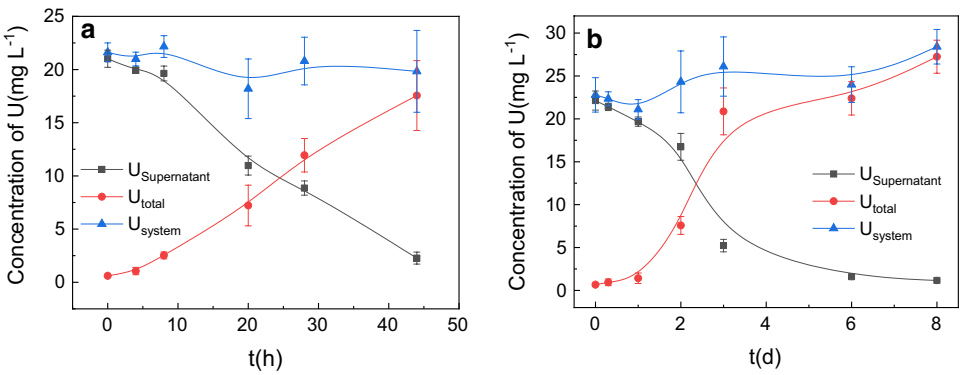

Fig. 2 The concentrations of $U_{supernatant}$, U_{total}, and U_{system} in the U(VI) immobilization process by *S. putrefaciens* (**a**) and AnGS (**b**)

U speciation and distribution in microbial aggregates

In this study, the U distribution in four fractions of microbial aggregates, which represented four main forms by microorganisms can immobilize U, was analyzed. The four fractions are set as (1) extracellular EPS-combined U, (2) extracellular non-reductive and mineralized U(VI) (as EPS were previously extracted, soluble U(VI) through biosorption could be little and mainly U(VI) minerals was in 100 mM $NaHCO_3$ extracts), (3) extracellular microbially mediated reductive U(IV) precipitation, and (4) intracellular U. During U(VI) immobilization process by microorganisms in all tests, the concentration of each fraction of U (U_{EPS}, $U_{VI\text{-}EX}$, $U_{IV\text{-}EX}$ and U_{IN}) as time went on was analyzed (Fig. 3 and Table 1). The percentage value of each U fraction in the microorganisms calculated by U/U_{total} is shown in Table 2.

The first U fraction immobilized by microorganisms was extracellular EPS-combined U. EPS were extracellular macromolecule substances secreted by microorganisms, which might play important roles in the reaction of U(VI) and microorganisms. Under toxic conditions, microorganisms might secrete more EPS to form a protective layer, adsorbing or binding those toxic substances. The toxicity of metals is related to the activity of free metallic ions, when metals are complexed or adsorbed by organic or inorganic ligands, their toxicity to microorganisms is greatly reduced [30]. As EPS were the first barrier facing U(VI) before U(VI) diffusing through EPS and reacting with cells, the ability to accumulate U should be one of the important properties for EPS [17]. It can be seen in Fig. 3 that EPS had accumulated a large amount of U in this experiment. As for *S. putrefaciens* and AnGS, the contribution of EPS to U(VI) immobilization were respectively 11.8 ± 1.1% and 8.8 ± 1.1% (Table 2) at the end. Similar effects have been reported in studies on metal ion immobilization [22]. Approximate contribution of EPS to U removal has been achieved in our previous study using AnGS [23], though different methods were applied to extract EPS. Overall, a small percentage of U was indeed accumulated in EPS. Details about the species of U in EPS were discussed below.

The second U fraction immobilized by microorganisms was extracellular non-reductive U(VI) mineralization, which was shown as $U_{VI\text{-}EX}$ in Fig. 3. The non-reductive U(VI)

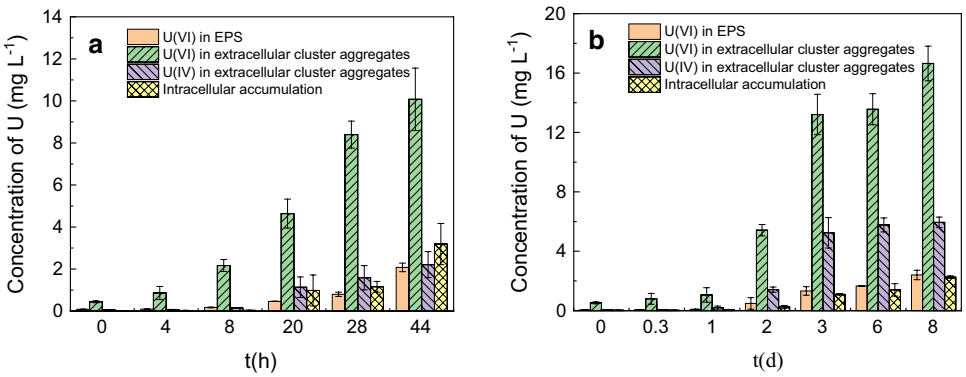

Fig. 3 The concentrations of U_{EPS}, $U_{VI\text{-}EX}$, $U_{IV\text{-}EX}$ and U_{IN} in the U(VI) immobilization process by *S.putrefaciens* (**a**) and AnGS (**b**)

Table 1 The U fractions and their contents in the *S. putrefaciens* and AnGS

Test	Time	U_{EPS} Content (mg L^{-1})	$U_{VI\text{-}EX}$ Content (mg L^{-1})	$U_{IV\text{-}EX}$ Content (mg L^{-1})	U_{IN} Content (mg L^{-1})
S. putrefaciens	0	0.086 ± 0.005	0.44 ± 0.046	0.055 ± 0.014	0.023 ± 0.003
	4 h	0.093 ± 0.012	0.86 ± 0.31	0.070 ± 0.011	0.029 ± 0.010
	8 h	0.17 ± 0.015	2.17 ± 0.28	0.15 ± 0.021	0.038 ± 0.010
	20 h	0.46 ± 0.0016	4.64 ± 0.69	1.14 ± 0.49	0.98 ± 0.73
	28 h	0.80 ± 0.10	8.40 ± 0.64	1.59 ± 0.58	1.15 ± 0.25
	44 h	2.08 ± 0.20	10.08 ± 1.48	2.21 ± 0.62	3.19 ± 0.98
AnGS	0	0.053 ± 0.005	0.52 ± 0.068	0.051 ± 0.011	0.027 ± 0.005
	0.3 d	0.063 ± 0.008	0.79 ± 0.36	0.057 ± 0.016	0.028 ± 0
	1 d	0.089 ± 0.009	1.05 ± 0.48	0.21 ± 0.099	0.064 ± 0.014
	2 d	0.48 ± 0.39	5.4 ± 0.38	1.41 ± 0.17	0.255 ± 0.095
	3 d	1.32 ± 0.28	13.2 ± 1.36	5.24 ± 1.02	1.09 ± 0.057
	6 d	1.66 ± 0.007	13.5 ± 1.04	5.77 ± 0.46	1.39 ± 0.41
	8 d	2.40 ± 0.31	16.6 ± 1.16	5.94 ± 0.35	2.25 ± 0.086

Table 2 The U fractions and their percentage in the *S. putrefaciens* and AnGS

Test	Time	U_{EPS} Fraction (%)	U_{VI-EX} Fraction (%)	U_{IV-EX} Fraction (%)	U_{IN} Fraction (%)
S. putrefaciens	0	14.1 ± 0.9	73.0 ± 7.7	9.1 ± 2.4	3.7 ± 0.6
	4 h	8.8 ± 1.2	81.8 ± 29.4	6.6 ± 1.0	2.7 ± 0.9
	8 h	6.9 ± 0.6	85.7 ± 11.2	5.9 ± 0.8	1.5 ± 0.3
	20 h	6.4 ± 0.02	64.2 ± 9.5	15.7 ± 6.7	13.5 ± 10.1
	28 h	6.4 ± 0.8	70.3 ± 5.3	13.3 ± 4.8	9.7 ± 2.1
	44 h	11.8 ± 1.1	57.4 ± 8.4	12.5 ± 3.5	18.1 ± 5.5
AnGS	0	9.0 ± 0.8	79.1 ± 10.3	7.6 ± 1.6	4.1 ± 0.8
	0.3 d	6.7 ± 0.8	84.2 ± 38.4	6.0 ± 1.7	2.9 ± 0.02
	1 d	6.2 ± 0.6	74.4 ± 34.4	14.7 ± 7.0	4.5 ± 1.0
	2 d	6.4 ± 5.1	71.5 ± 5.0	18.6 ± 2.3	3.3 ± 1.2
	3 d	6.3 ± 1.3	63.2 ± 6.5	25.1 ± 4.9	5.2 ± 0.2
	6 d	7.4 ± 0.03	60.5 ± 4.6	25.7 ± 2.0	6.2 ± 1.8
	8 d	8.8 ± 1.1	61.1 ± 4.2	21.8 ± 1.2	8.2 ± 0.3

mineralization represented the process that U(VI) immobilized by microorganisms but not receive electrons, involving biosorption (U(VI) adsorption by microorganisms and binding in the functional group of bacteria) and mineralization (U(VI) mineralized with enzymatically-generated ligands due to a phosphatase activity). It can be seen that non-reductive U(VI) mineralization was the main mechanism of microbial immobilization of U. Since the cell surface, including cell wall, directly contacted with the environment, the charged groups within the surface layers were able to interact with ions or charged molecules present in the external milieu. Under neutral conditions, the speciation of U(VI) was dominated by stable complexes such as hydroxides or carbonates [17]. Based on thermodynamic simulation, uranyl hydroxide, uranyl carbonate and calcium-U carbonate species could form stable surface complexes on microbial cells [31]. In addition of functional groups, phosphatase also played an important role in the microbial non-reductive mineralization of U [32]. Over expression of bacterial phosphatase induced by heavy metal stimulation could be used as a detoxification mechanism of bacteria themselves. The intracellular phosphatase could produce phosphates under the stimulation of U(VI), thus promoting better fixation of U, which could reduce the toxicity of U(VI) to cells. Islam et al. [33] isolated a variety of bacteria from U mines and studied their interaction with U, and found that most of them could immobilize U into U phosphate compounds or uranyl phosphate hydrates in phosphorus-free solutions. It was hypothesized that these bacteria might induce the immobilization of uranyl ions by increasing the concentration of surrounding phosphate under the action of phosphatase. Therefore, the U(VI) in the extracellular cluster aggregates in this study might mainly be composed of uranyl carbonate and uranyl phosphate complexes. Under the experimental conditions in this study, the contributions of non-reductive mineralization to U(VI) immobilization of *S.putrefaciens* and AnGS were 57.4 ± 8.4% and 61.1 ± 4.2% (Table 2) at the end, respectively.

U_{IV-EX} concentrations in Fig. 3 represented the microbially mediated reductive precipitation of U(VI) to U(IV). Bioreduction mainly refers to the reduction of soluble U(VI) to insoluble U(IV) through special enzymatic action of microorganisms under anaerobic conditions [15]. *S. putrefaciens* could use U(VI) as the terminal electron acceptor of energy metabolism. AnGS had highly specific microbial biodiversity that was capable of U(VI) bioreduction [14]. Bioreduction could be influenced by environmental factors. Some coexisting ions such as Ca^{2+}, Mg^{2+}, CO_3^{2-} and NO_3^- have been reported to have obvious inhibitory effect on U reduction by microorganisms [34, 35]. The contents of U(IV) in *S. putrefaciens* were from the initial 0.055 ± 0.014 mg L^{-1} to the last 2.21 ± 0.62 mg L^{-1}(Fig. 3a and Table 1), and in the AnGS from 0.051 ± 0.011 to 5.94 ± 0.35 mg L^{-1} (Fig. 3b and Table 1). Results showed that *S. putrefaciens* and AnGS had the ability to reduce U(VI), and the maximum contribution of reduced U(IV) to total U removal by *S. putrefaciens* and AnGS under ambient conditions were 12.5 ± 3.5% and 21.8 ± 1.2% (Table 2) at the end, respectively. Notably, the proportion of biological reduction for *S. putrefaciens* was relatively small, probably because the presence of bicarbonate ions inhibited or significantly decreased the bioreduction of U(VI) by microorganisms [36].

U_{IN} concentrations in Fig. 3 represented the intracellular accumulated U in microorganisms. It can be seen from Table 2 that the contribution of intracellular accumulation to total U removal by *S. putrefaciens* and AnGS was respectively 18.1 ± 5.5% and 8.2 ± 0.3% at the end. Unlike essential metals such as iron, zinc and manganese, which are accumulated intracellularly through metabolic systems. Some studies have found that the accumulation of U inside

microorganisms was due to the increased membrane permeability caused by the toxicity of U, and the chelation of polyphosphate with U inside microorganisms [37].

During U(VI) immobilization process by microorganisms in all tests, U(IV)/U(VI) ratios were calculated, and variations of which in microbial aggregates during the process are shown in Fig. 4. In all tests with U(VI) added, U(IV)/U(VI) ratios decreased after reaction, then gradually increased as time went on. The ratios of U(IV)/U(VI) in AnGS were relatively higher than that in *S. putrefaciens*, which may be that there were many kinds of U reducing bacteria in AnGS. The AnGS was taken out from the storage condition of 4 °C for tests, its U reducing activity needed to be stimulated for a period, resulting that the ratios of U(IV)/U(VI) were similar to *S. putrefaciens* in the first 1 d. After 1 d, the reduction of U(VI) to U(IV) increased rapidly. Taken results of U(IV)/U(VI) ratios, it could be concluded that most U(VI) was combined to microorganisms through adsorption or complexation before reduction to U(IV) and U(VI) immobilization was much faster than U(VI) bioreduction.

Contents and forms of U in the EPS

Fractions of soluble and particulate U in EPS, and also size distribution of particulate U are shown in Table 3 and Fig. 5. The forms of U in EPS of *S. putrefaciens* and AnGS displayed different characteristics. For *S. putrefaciens*, more than 35% of U was present as soluble ions in the whole process, and this fraction could be over 50% in the initial 4 h. While U in the EPS of AnGS was mainly present in the form of nano-sized particles, accounting for over 80% nearly all the time (Table 3). Both fractions of soluble U in EPS for *S. putrefaciens* and AnGS were significantly increased in the initial stage of the reaction and then gradually decreased over time. This phenomenon demonstrated that mainly biosorption of uranyl ions by EPS occurred in the initial period and then the soluble ions would be consumed to form U particles. Results showed that U immobilization in EPS mainly through biosorption for *S. putrefaciens*, while mainly bioprecipitation for AnGS. The presence of higher density of ions like phosphorus in the EPS of AnGS might promote the formation of U precipitates.

The particle size distribution of U in EPS varied with time. U particles in EPS of *S. putrefaciens* gradually formed and grew larger over time, with concentrations increasing from 4 766 ± 278 parts mL^{-1} to 84 000 ± 3 784 parts mL^{-1} and mean size from 11.4 ± 0.9 to 163.1 ± 5.8 nm (Table 3 and Fig. 5a, b). U particles in EPS of AnGS increased from 35 300 ± 1 357 parts mL^{-1} to 232,698 ± 7 445 parts mL^{-1}, and the mean size increased from 16.7 ± 1.0 to 128.4 ± 4.2 nm (Table 3 and Fig. 5c, d). Results of the mean size of U particles in *S. putrefaciens* and AnGS tests were analyzed using analysis of variance (ANOVA) method. According to ANOVA analysis, insignificant difference is

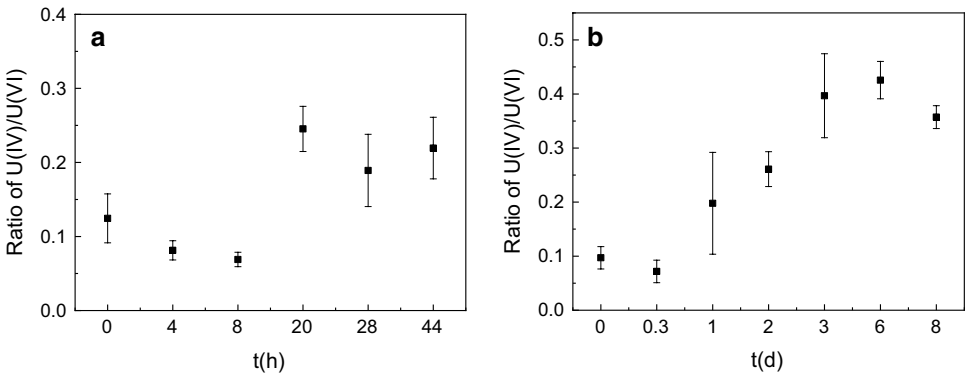

Fig. 4 Variations of ratios of U(IV)/U(VI) in the time course of U(VI) immobilization by *S.putrefaciens* (**a**) and AnGS (**b**)

Table 3 Fractions of soluble and particulate U and size distribution of particulate U in EPS extracts detected by ICP-MS (diluted 20 times)

Test	Time	Soluble (%)	Particulate (%)	Mean size (nm)	Particle concentration (parts mL^{-1})
S. putrefaciens	0	53.7 ± 3.2	46.3 ± 2.7	11.4 ± 0.9	4766 ± 278
	4 h	84.5 ± 5.1	15.5 ± 0.9	84.1 ± 3.7	3072 ± 160
	20 h	49.0 ± 3.0	51.0 ± 4.2	132.2 ± 6.2	71,240 ± 4421
	44 h	36.4 ± 1.3	63.6 ± 5.1	163.1 ± 5.8	84,000 ± 3784
AnGS	0	8.52 ± 1.4	91.5 ± 3.6	16.7 ± 1.0	35,300 ± 1357
	1 d	20.4 ± 1.0	79.6 ± 4.9	61.8 ± 3.2	18,686 ± 2870
	3 d	14.1 ± 0.8	85.9 ± 5.3	109.7 ± 2.9	71,783 ± 3895
	8 d	8.98 ± 0.8	91.0 ± 3.5	128.4 ± 4.2	232,698 ± 7445

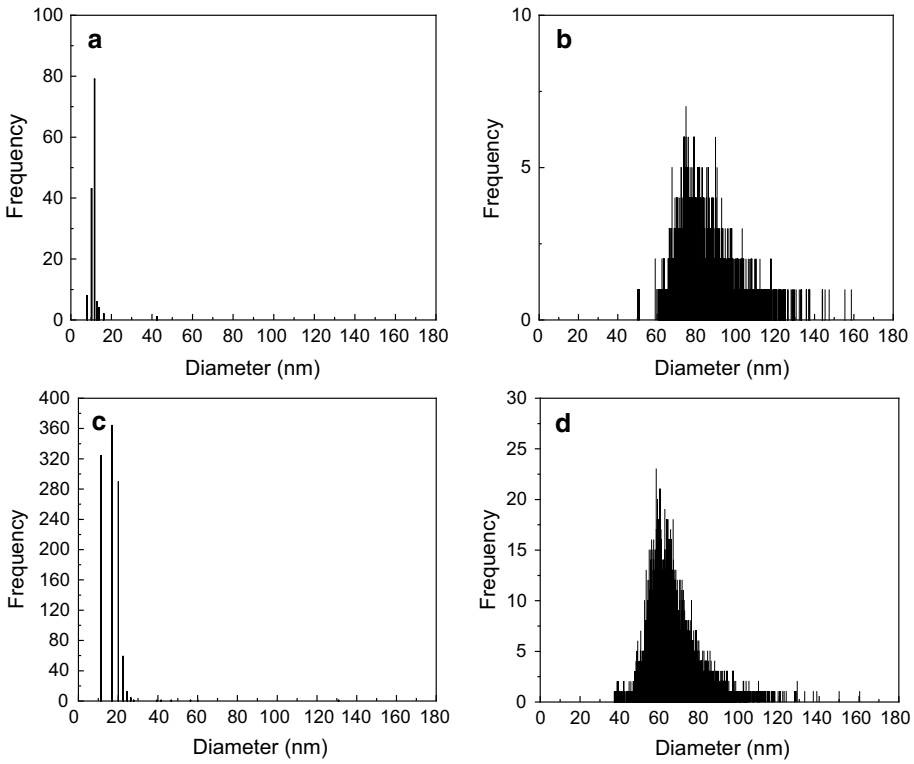

Fig. 5 Size distribution of nano-sized U particles in EPS extracts (diluted 100 times, each frequency equals to particle concentration of about 36.1 parts per mL). **a** *S. putrefaciens*, time = 0; **b** *S. putrefaciens*, time = 44 h; **c** AnGS, time = 0; **d** AnGS, time = Day 8

present in the U particle size of EPS between *S. putrefaciens* and AnGS ($P = 0.432 > 0.05$). Especially, in the initial stage of U(VI) immobilization by the two microbial aggregates, the amounts of U particles in EPS decreased and the mean diameter increased with only a little increase in the U content in EPS, demonstrating that smaller U particles aggregated and grew larger. This result was consistent with the previous results of EPS content determination, indicating that U accumulated in EPS over time. As reported by Jroundi et al. [38], U could precipitate in cell walls and EPS of *Myxococcusxanthus*.

Above results indicated that after the reaction with U(VI), both EPS of *S. putrefaciens* and AnGS were enriched with uranyl ions and U(VI) minerals. Biosorption and biomineralization were confirmed to be involved in the U(VI) immobilization by EPS.

Microscopic analysis of microbial aggregates

In order to further verify the accumulation of U in microbial aggregates, the morphologies and elements of *S. putrefaciens* and AnGS before and after exposure to U(VI) were analyzed by SEM coupled with EDX (Fig. 6). As shown, the *S. putrefaciens* cells were round, smooth and well-formed before reaction with U(VI) (Fig. 6a), while their surface shrinked after reaction with U(VI) (Fig. 6c). Many particles were found to be deposited on the surface of cells, which were confirmed to be U particles (Fig. 6d). These U particles may form by precipitation with phosphate groups released by cells. As reported by Vaideeswaran et al. [15], inorganic phosphate was released by cells, providing ligands for formation of insoluble U(VI) phosphates. Moreover, much EPS were produced after reaction with U and obviously observed coating on the surface of cells, which might explain the significant U immobilization by EPS (Fig. 3).

The SEM images of AnGS before and after U(VI) reaction are shown in Fig. 6e and g. Notably, the surface of AnGS was rough and irregular, and EPS were found coating on the surface of microorganism and filling in the gaps of microorganism (Fig. 6e). It can be seen in Fig. 6g that the surface of AnGS looks more smoother after reaction, and much EPS were produced on the surface of microorganism. This mainly might be due to the large secretion of EPS when facing high concentration of U(VI), which changed its surface morphology. There was no element U in the AnGS before reaction (Fig. 6f), but the absorption peak of element U appeared after reaction (Fig. 6h), indicating that a large amount of U were immobilized by AnGS.

FTIR analysis

FTIR was used to characterize the functional groups of microorganisms with scanning range of 400–4000 cm^{-1}. The FTIR spectra of *S. putrefaciens* and AnGS before and after reaction with U(VI) is shown in Fig. 7. The main functional groups and peaks of FTIR analysis were

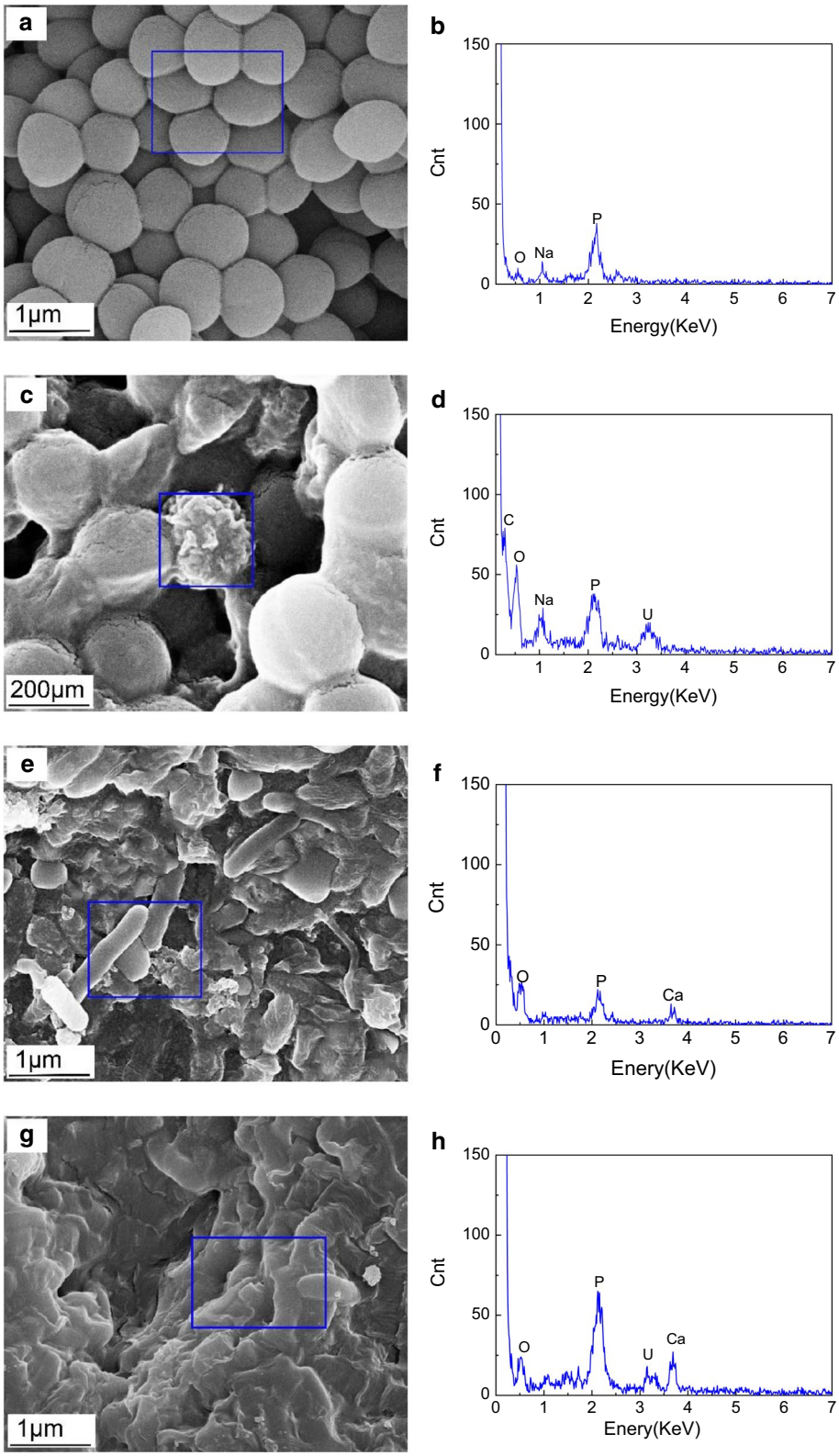

Fig. 6 SEM-EDX spectra of bacterial: original *S. putrefaciens* (**a**, **b**); U-loaded *S. putrefaciens* (**c**, **d**); original AnGS (**e**, **f**); U-loaded AnGS (**g**, **h**)

according to literatures [27, 39] and shown in Tables 4 and 5. As shown, some FTIR peaks of *S. putrefaciens* moved after their reaction with U(VI). The peaks at 2928 cm^{-1}, 1545 cm^{-1}, 1407 cm^{-1} and 559 cm^{-1} shifted to 2923 cm^{-1}, 1535 cm^{-1}, 1401 cm^{-1} and 615 cm^{-1}, respectively (Table 4). The 1049 cm^{-1} absorption band intensity weakened after reaction, indicating a coordination of uranyl to phosphoryl groups. These changes should be attributed to the

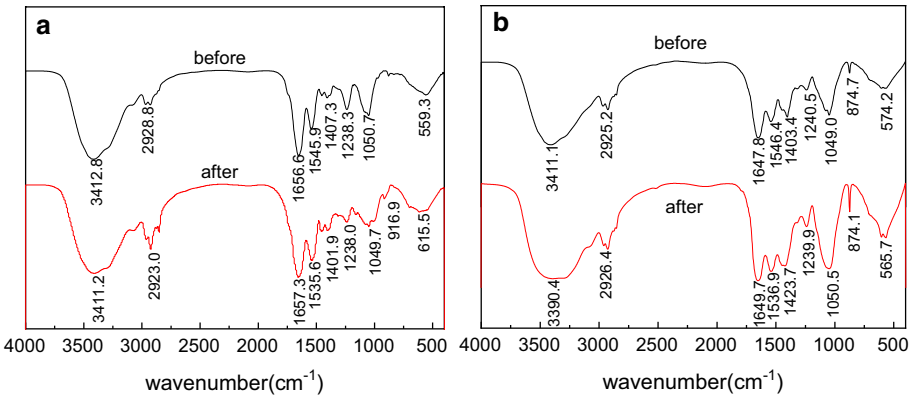

Fig. 7 FTIR spectra of *S. putrefaciens* (**a**) and AnGS (**b**) before and after reaction with U(VI)

Table 4 FTIR analysis of *S. putrefaciens* before and after reaction with U(VI)

Wavenumber before reaction (cm^{-1})	Wavenumber after reaction (cm^{-1})	Wavenumber range (cm^{-1})	Major functional groups
3412	3411	3700–3000	Stretching vibrations of –OH and $–NH_2$
2928	2923	3000–2900	C–H stretching vibration of methylene (–CH–)
1656	1657	1680–1630	Amide I, carbonyl (C=O) stretching vibration
1545	1535	1630–1540	Amide II, C–N stretching vibration, N–H bending vibration
1407	1401	1500–1250	Deformation vibrations of –OH
1050	1049	1200–850	Phosphate asymmetric and symmetric stretching bands
	916		Asymmetric stretching vibration of uranyl ions
559	615	< 800	Sstretching vibration of –C–X

Table 5 FTIR analysis of AnGS before and after reaction with U(VI)

Wavenumber before reaction (cm^{-1})	Wavenumber after reaction (cm^{-1})	Wavenumber range (cm^{-1})	Major functional groups
3411	3390	3700–3000	Stretching vibrations of –OH and $–NH_2$
2925	2926	3000–2900	C–H stretching vibration of methylene (–CH–)
1647	1649	1680–1630	Amide I, carbonyl (C=O) stretching vibration
1546	1536	1630–1540	Amide II, C–N stretching vibration, N–H bending vibration
1403	1423	1500–1250	Deformation vibrations of –OH
1049	1050	1200–850	Phosphate asymmetric and symmetric stretching bands
574	565	< 800	Stretching vibration of –C–X

interactions of groups on *S. putrefaciens* and the uranyl ions. The appearance of new peak at about 916 cm^{-1} was assigned to the asymmetric stretching vibration of uranyl ions, which indicated that the uranyl ions were successfully chelated by *S. putrefaciens* [40]. In summary, the changes of peak position demonstrated that there were strong coordination interactions between uranyl ions and carboxyl, phosphoryl and amide groups on the *S. putrefaciens* surface. Similarly, peaks of AnGS also moved after their reaction with U(VI) (Fig. 6b). Peaks at 3411 cm^{-1}, 1546 cm^{-1}, 1403 cm^{-1} and 574 cm^{-1} shifted to 3390 cm^{-1}, 1536 cm^{-1}, 1423 cm^{-1} and 565 cm^{-1}, respectively (Table 5). The 1049 cm^{-1} absorption band intensity enhanced after reaction, indicating a coordination of uranyl to phosphoryl groups. In the process of interactions between U and AnGS, carboxyl, phosphoryl and hydroxyl were the main reaction sites.

U immobilization mechanisms

Above results showed that the mechanisms of microbial immobilization of U were complex. Certain U in solution could be immobilized rapidly by the surface of cells and EPS, which contained numerous functional groups. Then, with its metabolism, such as enzymatic action, uranyl ions

were transformed into relatively stable states. In this study, four ways should be involved in the microbial immobilization of U, including the biosorption/complexation of soluble U by EPS and microbial cells (e.g. UO_2^{2+}, $UO_2(CO_3)_2^{2-}$ etc.), the formation of U(VI) precipitation through non-reductive biomineralization by EPS and microbial cells (e.g. U(VI)-phosphate precipitation, U(VI)-carbonate precipitation), bioreduction of soluble U(VI) to U(IV) precipitates (UO_2, or even U(IV)-phosphate) by EPS and microbial cells, and the intracellular accumulation of U. In addition, due to the special environmental geochemical characteristics of U(VI), some coexisting ions, such as metal ions and anions, also had certain effects on microbial immobilization of U. This study explored the speciation and distribution of U in microorganisms in the presence of carbonate, and these information of U in microorganisms under other conditions needs further study.

Implications of this work

The present work clarifies the interactions between the two different microbial aggregates and U, and the overall results suggest high U accumulation. The real applicability of the studied microorganisms in bioremediation processes should be evaluated in future, and then further management of microorganisms loaded with U also should be paid attention. Inorganic acid solution would be capable of effectively stripping the immobilized U from the microorganisms. Safety of the waste biomass and recovery of the loaded U could be both achieved.

A lot of studies have been reported about the remediation of a single radical element pollution in groundwater, while relatively little information is available on the remediation of multiple radionuclide pollution. Actually, thorium is also an important natural radioactive element in nature, which could form compound pollution with U in the environment. Previous investigations have shown that different kinds of microorganisms have excellent accumulation properties for thorium in groundwater [41]. The presence of thorium or other nuclides may affect the immobilization of U by microorganisms. Further work is needed to investigate the immobilization behavior of various nuclide ions by microorganisms.

Conclusions

The results presented here reported the speciation and distribution of U in microbial aggregates and the contribution of different mechanisms to U immobilization. Results showed that the interaction between microorganisms and U(VI) was complex. Non-reductive biomineralization was the main mechanism of microbial immobilization of U, and its maximum contribution to U removal by *S. putrefaciens* and AnGS were $57.4 \pm 8.4\%$ and $61.1 \pm 4.2\%$, respectively. As well, the contributions of EPS, bioreductive and intracellular accumulation could not be ignored. Both soluble and particulate U was detected in EPS analyzed by single particle ICP-MS, confirmed that biosorption and biomineralization occur in the process of U(VI) immobilization by EPS. In addition, SEM–EDX analysis showed that the presence of high content of U might promote the secretion of EPS and U subsequently combined to the released EPS to form U particles. FTIR analysis further demonstrated that uranyl ions were bonded to different functional groups of microorganisms. Overall, our results provided new insights into understanding and utilizing different mechanisms of microbial removal of U.

Authors' contributions F-CY, SF and H-X Huang designed experiments, and F-YH and H-LZ directed experiments and wrote the manuscript. Y-PW and M-XC performed experiments. J-C, W-JY and JZ helped with the experimentation. All authors read and approved the final manuscript.

Funding This study was funded by the National Natural Science Foundation of China (21571163, 21407133, 41402248 and 51608498), the key research and development projects of Sichuan science and technology department (No: 2018SZ0298), the science and technology planning projects of Panzhihua science and technology bureau (No. 2017CY-N-8), the Longshan academic research talent support program of Southwest University of Science and Technology (Nos. 17LZX308, 17LZX613, 18LZX638 and 18LZXT03) and the Scientific research project of Sichuan education department (No. 16ZB0150), Nuclear Facility Decommissioning and radioactive waste treatment research project of the State Administration of science, technology and industry of national defense (No. 1521 [2018] of the second division of science and Technology), Southwest University of Science and Technology Natural Science Foundation (No.18zx7125).

Compliance with ethical standards

Conflict of interest The authors declare that they have no competing interests.

Ethics approval All applicable international, national, and/or institutional guidelines for the care and use of animals were followed.

Consent for publication All authors gave their consent for publication.

References

1. Thomas B, Ruben K, Andreas K, Philippe VC, Matthew GV, Andreas V, Kate C (2009) Biogeochemical redox processes and their impact on contaminant dynamics. Environ Sci Technol 44:15–23
2. Liu P, Yu Q, Xue Y, Chen J, Ma F (2020) Adsorption performance of U(VI) by amidoxime-based activated carbon. J Radioanal Nucl Chem. https://doi.org/10.1007/s10967-020-07111-x
3. Wei H, Dong F, Chen M, Zhang W, He M, Liu M (2020) Removal of uranium by biogenetic jarosite coupled with

photoinduced reduction in the presence of oxalic acid: a low-cost remediation technology. J Radioanal Nucl Chem. https://doi.org/10.1007/s10967-020-07125-5
4. Newsome L, Morris K, Lloyd JR (2014) The biogeochemistry and bioremediation of uranium and other priority radionuclides. Chem Geol 363:164–184
5. Spear JR, Figueroa LA, Honeyman BD (1999) Modeling the removal of uranium U(VI) from aqueous solutions in the presence of sulfate reducing bacteria. Environ Sci Technol 33:2667–2675
6. Finneran KT, Anderson RT, Nevin KP, Lovley DR (2002) Potential for bioremediation of uranium-contaminated aquifers with microbial U(VI) reduction. J Soil Contam 11:339–357
7. Anderson RT, Vrionis HA, Ortiz-Bernad I, Resch CT, Long PE, Dayvault R, Karp K, Marutzky S, Metzler DR, Peacock A, White DC, Lowe M, Lovley DR (2003) Stimulating the in situ activity of geobacter species to remove uranium from the groundwater of a uranium-contaminated aquifer. Appl Environ Microbiol 69:5884–5891
8. Renshaw JC, Lloyd JR, Livens FR (2003) Microbial interactions with actinides and long-lived fission products. C R Chim 10:1067–1077
9. Lovley DR, Phillips EJP, Gorby YA, Landa ER (1991) Microbial reduction of uranium. Nature 350:413–416
10. Mumtaz S, Streten-Joyce C, Parry DL, Mcguinness KA, Lu P, Gibb KS (2013) Fungi outcompete bacteria under increased uranium concentration in culture media. J Environ Radioact 120:39–44
11. Sheng L, Fein JB (2014) Uranium reduction by Shewanella oneidensis MR-1 as a function of $NaHCO_3$ concentration: surface complexation control of reduction kinetics. Environ Sci Technol 48:3768–3775
12. Newsome L, Morris K, Lloyd JR (2015) Uranium biominerals precipitated by an environmental isolate of serratia under anaerobic conditions. PLoS ONE 10:1–14
13. Nancharaiah YV, Joshi HM, Mohan TVK, Venugopalan VP, Narasimhan SV (2006) Aerobic granular biomass: a novel biomaterial for efficient uranium removal. Curr Sci 91:503–509
14. Tapia-Rodriguez A, Luna-Velasco A, Field JA, Sierra-Alvarez R (2010) Anaerobic bioremediation of hexavalent uranium in groundwater by reductive precipitation with methanogenic granular sludge. Water Res 44:2153–2162
15. Vaideeswaran S, Maxim IB, Brent MP, Sridhar V, Robin G, William AA, Rajesh KS, Alice D, Kenneth MK, Thomas B (2011) Multiple mechanisms of uranium immobilization by *cellulomonas* sp. strain es6. Biotechnol Bioeng 108:264–276
16. Lloyd JR, Macaskie LE (2002) Chapter 11 biochemical basis of microbe-radionuclide interactions. Radioact Environ 2:313–342
17. Merroun ML, Selenska-Pobell S (2008) Bacterial interactions with uranium: an environmental perspective. J Contam Hydrol 102:285–295
18. Zhao C, Jun L, Li X, Li F, Tu H, Sun Q, Liao J, Yang J, Yang Y, Liu N (2016) Biosorption and bioaccumulation behavior of uranium on *Bacillus* sp. dwc-2: investigation by Box-Behenken design method. J Mol Liq 221:156–165
19. Merroun M, Nedelkova M, Rossberg A, Hennig C, Scheinost AC, Selenska-pobell S (2006) Interaction mechanisms of uranium with bacterial strains isolated from extreme habitats. Spec Publ R Soc Chem 305:47–49
20. Macaskie L, Empson R, Cheetham A, Grey C, Skarnulis A (1992) Uranium bioaccumulation by a *citrobacter* sp. as a result of enzymically mediated growth of polycrystalline HUO_2PO_4. Science 257:782–784
21. Newsome L, Morris K, Trivedi D, Bewsher AD, Lloyd JR (2015) Biostimulation by glycerol phosphate to precipitate recalcitrant uranium(IV) phosphate. Environ Sci Technol 49:11070–11078
22. Cao B, Ahmed B, Kennedy DW, Wang Z, Shi L, Marshall MJ, Fredrickson JK, Isern NG, Majors PD, Beyenal H (2011) Contribution of extracellular polymeric substances from *Shewanella* sp. HRCR-1 biofilms to U(VI) immobilization. Environ Sci Technol 45:5483–5490
23. Zhang H, Cheng M, Liu W, Huang F, Ding H, Li S, Guo W, Wang Y, Huang H (2017) Characterization of uranium in the extracellular polymeric substances of anaerobic granular sludge used to treat uranium-contaminated groundwater. RSC Adv 7:54188–54195
24. Haas JR, Dichristina TJ, Wade R Jr (2001) Thermodynamics of U(VI) sorption onto *Shewanella putrefaciens*. Chem Geol 180:33–54
25. Vogt SJ, Stewart BD, Seymour JD, Peyton BM (2012) Detection of biological uranium reduction using magnetic resonance. Biotechnol Bioeng 109:877–883
26. Luo W, Wu WM, Yan T, Criddle CS, Jardine PM, Zhou J, Gu B (2007) Influence of bicarbonate, sulfate, and electron donors on biological reduction of uranium and microbial community composition. Appl Microbiol Biotechnol 77:713–721
27. Huang W, Nie X, Dong F, Ding C, Huang R, Qin Y, Liu M, Sun S (2017) Kinetics and pH-dependent uranium bioprecipitation by *Shewanella putrefaciens* under aerobic conditions. J Radioanal Nucl Chem 312:531–541
28. Elias DA, Senko JM, Krumholz LR (2003) A procedure for quantitation of total oxidized uranium for bioremediation studies. J Microbiol Methods 53:343–353
29. Suzuki Y, Tanaka K, Kozai N, Ohnuki T (2010) Effects of citrate, NTA, and EDTA on the reduction of U(VI) by *Shewanellaputrefaciens*. Geomicrobiol J 27:245–250
30. Ke MH, Murgel GA, Lion LW, Shuler ML (1994) Interactions of microbial biofilms with toxic trace metals: 2. Prediction and verification of an integrated computer model of lead(II) distribution in the presence of microbial activity. Biotechnol Bioeng 44:232–239
31. Drew GL, Elias PE, Fein JB (2005) Adsorption of aqueous uranyl complexes onto Bacillus subtilis cells. Environ Sci Technol 39:4906–4912
32. Merroun ML, Nedelkova M, Ojeda JJ, Reitz T, LópezFernández M, Arias JM, MaríaRomero-González S-PS (2011) Bio-precipitation of uranium by two bacterial isolates recovered from extreme environments as estimated by potentiometric titration, TEM and X-ray absorption spectroscopic analyses. J Hazard Mater 197:1–10
33. Islam E, Sar P (2016) Diversity, metal resistance and uranium sequestration abilities of bacteria from uranium ore deposit in deep earth stratum. Ecotoxicol Environ Saf 127:12–21
34. Finneran KT, Housewright ME, Lovley DR (2002) Multip, le influences of nitrate on uranium solubility durin ~ 1 bioremediation of uranium-contaminated subsurface sediments. Environ Microbiol 4:510–516
35. Brooks SC, Fredrickson JK, Carroll SL, KennedyD W (2003) Inhibition of bacterial U(VI) reduction by Calcium. Environ Sci Technol 37:1850–1858
36. Belli KM, Dichristina TJ, Cappellen PV, Taillefert M (2015) Effects of aqueous uranyl speciation on the kinetics of microbial uranium reduction. Geochim Cosmochim Acta 157:109–124
37. Suzuki Y, Banfield JF (1999) Geomicrobiology of uranium. Rev Miner Geochem 38:393–432
38. Jroundi F, Merroun ML, Arias JM, Rossberg A, Selenska-Pobell S, González-Muñoz MT (2007) Spectroscopic and microscopic characterization of uranium biomineralization in *Myxococcusxanthus*. Geomicrobiol J 24:441–449
39. Liu F, Teng S, Song R, Wang S (2010) Adsorption of methylene blue on anaerobic granular sludge: effect of functional groups. Desalination 263:11–17
40. MüllerK BV, Foerstendorf H (2008) Aqueous uranium(VI) hydrolysis species characterized by attenuated total

reflection Fourier-transform infrared spectroscopy. Inorg Chem 47:10127–10134
41. Kazy SK, D'Souza SF, Sar P (2009) Uranium and thorium sequestration by a *Pseudomonas* sp.: mechanism and chemical characterization. J Hazard Mater 163(1):65–72